THE ADVANTAGE OF LIDAR DIGITAL TERRAIN MODELS IN DOLINE MORPHOMETRY COMPARED TO TOPOGRAPHIC MAP BASED DATASETS – AGGTELEK KARST (HUNGARY) AS AN EXAMPLE

PREDNOST LIDARSKEGA DIGITALNEGA MODELA RELIEFA ZA RAZISKAVO MORFOMETRIJE VRTAČ V PRIMERJAVI S PODATKOVNO BAZO TOPOGRAFSKIH KART – PRIMER AGTELEŠKEGA KRASA (MADŽARSKA)

Tamás TELBISZ[1], Tamás LÁTOS[2], Márton DEÁK[3], Balázs SZÉKELY[4], Zsófia KOMA[5] & Tibor STANDOVÁR[6]

Abstract   UDC 551.435.82:528.8.044.6(439)
Tamás Telbisz, Tamás Látos, Márton Deák, Balázs Székely, Zsófia Koma & Tibor Standovár: The advantage of lidar digital terrain models in doline morphometry compared to topographic map based datasets – Aggtelek karst (Hungary) as an example
Doline morphometry has always been in the focus of karst geomorphological research. Recently, digital terrain model (DTM) based methods became widespread in the study of dolines. Today, LiDAR datasets provide high resolution DTMs, and automated doline recognition algorithms have been developed. In this paper, we test different datasets and a doline recognition algorithm using Aggtelek Karst (NE-Hungary) dolines as a case example. Three datasets are compared: "TOPO" dolines delineated by the classical outermost closed contour method using 1:10,000 scale topographic maps, "KRIG" dolines derived automatically from the DTM created by kriging interpolation from the digitized contours of the same topographic maps, and finally "LiDAR" dolines derived automatically from a DTM created from LiDAR data. First, we analyzed the sensitivity of the automatic method to the "depth limit" parameter, which is the threshold, below which closed depressions are considered as "errors" and are filled. In the actual case, given the typical doline size of the area and the resolution of the DTMs, we found

Povzetek   UDK 551.435.82:528.8.044.6(439)
Tamás Telbisz, Tamás Látos, Márton Deák, Balázs Székely, Zsófia Koma & Tibor Standovár: Prednost lidarskega digitalnega modela reliefa za raziskavo morfometrije vrtač v primerjavi s podatkovno bazo topografskih kart – primer Agteleškega krasa (Madžarska)
Morfometrija vrtač je bila vedno v središču kraških geomorfoloških raziskav. V zadnjem času so pri raziskavah vrtač postale zelo razširjene metode, ki temeljijo na digitalnem modelu reliefa (DMR). Lidarski podatki zagotavljajo visoko ločljivostne DMR-je, razviti so bili avtomatski algoritmi za prepoznavanje vrtač. V tem prispevku smo na primeru Agteleškega krasa v severovzhodni Madžarski preizkusili različne podatkovne baze in algoritme za prepoznavanje vrtač. Primerjali smo tri podatkovne baze: "TOPO" vrtače so razmejene na klasičen način z zunanjo zaprto plastnico na topografski karti v merilu 1: 10.000, "KRIG" vrtače so v istem merilu s pomočjo kriginga samodejno pridobljene iz digitaliziranih plastnic DMR, in "LiDAR" vrtače so samodejno pridobljene iz DMR, ki je ustvarjen iz lidarskih podatkov. Najprej smo analizirali občutljivost avtomatske metode parametra "mejne globine", ki predstavlja prag, pod katerim se depresijske oblike štejejo kot "napake" in so zapolnjene. V konkretnem primeru smo glede na običajno velikost vrtače in ločljivosti DMR ugotovili, da je optimalna

[1] Eötvös University Department of Physical Geography, 1117 Budapest, Pázmány sétány 1/C., Hungary, e-mail: telbisztom@caesar.elte.hu
[2] Eötvös University Department of Physical Geography, 1117 Budapest, Pázmány sétány 1/C., Hungary, e-mail: latostamas@gmail.cou
[3] Eötvös University Department of Physical Geography, 1117 Budapest, Pázmány sétány 1/C., Hungary, e-mail: dmarton@elte.hu
[4] Eötvös University Department of Geophysics and Space Science, 1117 Budapest, Pázmány P. sétány 1/C., Hungary; Department of Geodesy and Geoinformation, Vienna University of Technology, Gußhausstraße 27-29/E120, A-1040 Vienna, Austria; Interdiszplinäres Ökologisches Zentrum, TU Bergakademie Freiberg, Leipziger str. 29, D-09596 Freiberg, Germany, e-mail: balazs.szekely@ttk.elte.hu
[5] Eötvös University Department of Geophysics and Space Science, 1117 Budapest, Pázmány P. sétány 1/C., Hungary, e-mail: zsofia.koma@ttk.elte.hu
[6] Eötvös University Department of Plant Systematics, Ecology and Theoretical Biology, 1117 Budapest, Pázmány P. sétány 1/C., Hungary, e-mail: standy@caesar.elte.hu
Received/Prejeto: 02.02.2016

that ca. 0.5 m is the optimal depth limit for the LiDAR dataset and 1 m for the KRIG dataset. The statistical distributions of the morphometrical properties were similar for all datasets (lognormal distribution for area and gamma distribution for depth), but the DTM-based methodology resulted larger dolines with respect to the classical method. The planform area (and related characteristics) showed very high correlations between the datasets. Depth values were less correlated and the lowest (moderately strong) correlations were observed between circularity values of the different datasets. Slope histograms calculated from the LiDAR data were used to cluster dolines, and these clusters differentiated dolines similarly to the classical depth-diameter ratio. Finally, we conclude that in the actual case, dolines can be morphometrically well characterized even by the classical topographic method, though finer results can be achieved for the depth and shape related parameters by using LiDAR data.

Key words: doline morphometry, LiDAR, interpolation, slope histogram, sink point.

globinska meja za LiDAR ca. 0,5 m in 1 m za KRIG. Pri vseh podatkovnih bazah so bile statistične porazdelitve morfometrijskih lastnosti (logaritemska normalna porazdelitev za prostor in gama porazdelitev za globino) podobne, vendar metodologija, ki temelji na DMR privede do rezultatov, ki kažejo na večje vrtače v primerjavi s klasično metodo. Rezultati območij vrtač (in njihovih značilnosti) so pokazali zelo visoke korelacije med podatkovnimi nizi. Pri globinah so bile korelacije manjše in najnižje zabeležene korelacije (srednje močne) so bile med podatki različnih podatkovnih bazah. Histogrami naklona, izračunani iz lidarskih podatkov, so bili uporabljeni za združevanje vrtač, in ti grozdi razlikujejo vrtače glede na klasično razmerje med globino in premerom. Na koncu smo ugotovili, da lahko v konkretnem primeru dobro določimo morfometrične lastnosti vrtač s klasičnimi topografskimi metodami. Podrobnejše rezultate o globinah in oblikah lahko dosežemo na podlagi lidarskih podatkov.

Ključne besede: morfometrija vrtač, LiDAR, interpolacija, histogram naklona, ponor.

INTRODUCTION

Dolines are the diagnostic landforms of karst landscapes as cited so many times (Ford & Williams 1989). That is why the study of dolines is fundamental in karstology. Although there is an agreement in the basic types of dolines, there exist many categorizations of dolines principally based on their genesis (from Cvijič 1893 to Ford & Williams 1989; Šušteršič 1994; Gams 2000; Čar 2001; Sauro 2003). The morphometrical description of dolines started by the work of Williams (1971). Earlier morphometrical studies used aerial photos and topographic maps as well as field measurements (Vincent 1987; Kemmerly 1982, 1986; Mills & Starnes 1983; Bárány Kevei & Mezősi 1993). In many cases, the scale and quality of topographic maps limit the lowermost detectable doline size and the fidelity of doline shape representation (cf. Day 1983). On the other hand, field work is time consuming, that hampers the collection of bulk data appropriate for statistical analysis. It was an important step, when doline morphometry was integrated in a GIS framework (Orndorff *et al.* 2000; Denizman, 2003; Angel *et al.* 2004; Gao *et al.* 2005), that helped the recognition of spatial patterns and finding links between doline properties and other parameters, namely geology, structure (Faivre & Reiffsteck, 2002; Florea 2005; Telbisz *et al.* 2009, 2011; Pahernik 2012), glaciation (Plan & Decker 2006) or urban expansion (Brinkmann *et al.* 2008).

Since the 2000s, digital terrain models (DTMs) were also increasingly used in karst morphological analysis. A special goal of using DTMs is to find an automatic (or semi-automatic) method to derive dolines directly from DTMs. Earlier studies applied mainly contour-based DTMs (Telbisz *et al.* 2009; Pardo-Igúzquiza *et al.* 2013), or aerial stereo-photogrammetry (Zboray & Bárány Kevei 2004), but other data sources, such as SRTM or ASTER were also utilized for karst morphometry (Carvalho *et al.* 2013). More recently, LiDAR-based DTMs proved to be very useful due to their unprecedented high resolution, which lead to a boom in doline morphometrical studies (Gostinčar 2013; Obu & Podobnikar 2013; Rahimi & Alexander 2013; Gallay *et al.* 2013; Kobal *et al.* 2015; Zhu *et al.* 2014; Bauer 2015). We note, that there is also a much cheaper, concurrent method, the SfM (structure from motion), which is suitable to create high resolution DTMs, in case the vegetation is sparse, however we do not know any published report about the use of SfM in doline morphometrical studies.

There are at least three substantial questions with LiDAR-based doline recognition methods. The first question is, how precisely these methods can delineate dolines, and discriminate karst depressions from other types of depressions (real or artificial). Second, whether the earlier morphological results (shape properties, density, etc.) are in agreement with the results of LiDAR-based analysis. Third, what are the points, where we can expand our knowledge about doline morphology due to this new technology. Thus, the aim of this study is to present an automatic doline delineation method and answer these questions using the Aggtelek Karst as a case example.

DATA AND METHODOLOGY

STUDY AREA

The Aggtelek Karst is found in the north-eastern part of Hungary. It is mainly a hilly region, the highest point being only 604 m a.s.l. (Fertős-tető), but the relief is variegated (steep slopes, plateaus) due to karst features. Dolines are found both on the plateaus and in the valleys. Its cave systems together with the caves of Slovak Karst are part of the World Heritage. The karst terrain is predominantly built up of middle and upper Triassic karstifiable rocks (Wetterstein Limestone and Dolomite, Gutenstein Limestone and Dolomite, Steinalm Limestone; Less 1998). There were several paleokarst phases during the Cretaceous and early Tertiary, but most of the area was covered by non-karstic sediments during the Miocene. Since that time, the uplift of the Carpathians resulted that the still covered karst area became a pediment surface, and a valley network was formed on it (Zámbó 1998; Gaál & Bella 2005; Petrvalská 2010a; Telbisz 2011). As the uplift continued, more and more parts of the karst terrains were exhumed since the Pliocene, and some of the valleys were inherited on the karst surface and dolines were formed in these valleys from stream sinkpoints

(Jakucs 1956; Hevesi 1991; Móga 1999). Morphometry of Aggtelek Karst dolines have been studied by Mezősi (1984), Bárány-Kevei & Mezősi (1993), Telbisz (2001) and Veress (2008). Dolines of the neighbouring Slovak Karst were also in the focus of morphometrical studies (Petrvalská 2010b, 2012). Aggtelek Karst Dolines are almost exclusively of solutional origin, no collapse forms or subsidence dolines are present. Most of the dolines are covered with thin soil layer (with remnants of terra rossa type material at many sites), but doline fills may reach 5–10 m at depression centres (Zámbó 1998). At the foot of karst plateaus, some depressions are formed around sinking streams.

The present study area (Fig. 1) is 144.5 km² including most part of Aggtelek Karst (except the easternmost Szalonna Karst, where LiDAR data were not available). About half of this (73.1 km²) is the doline-dotted surface, for which the doline densities were calculated. This doline-dotted surface consists of 10 units. Further on, we note that dolines almost exclusively occur on terrains with less than 10° mean slope, which represents 64.5 % of the above mentioned doline-dotted surface units.
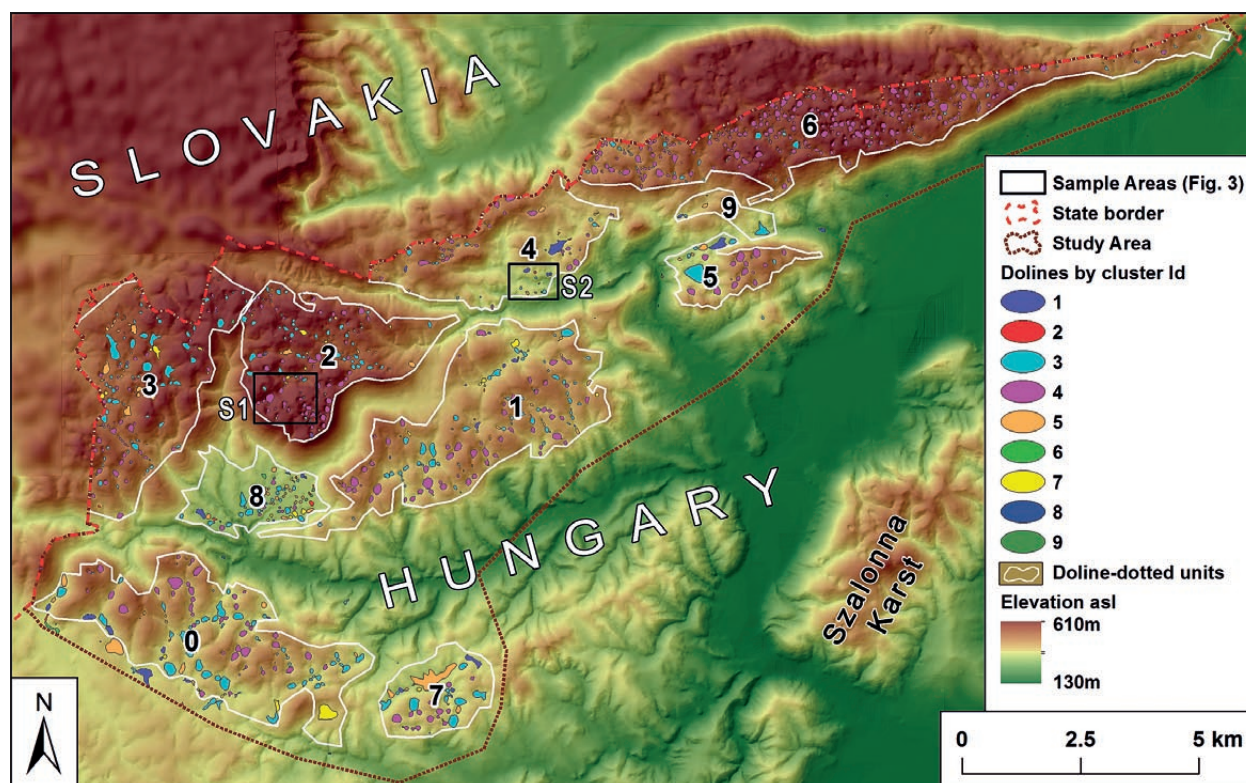

Fig. 1: The study area with the LiDAR-based dolines. Doline-dotted surface units (0-9) are delineated. Doline colours are according to slope-based clustering (for further explanation see the Results / Clustering section and Table 4). S1: sample area 1; S2: sample area 2 in Fig. 3.
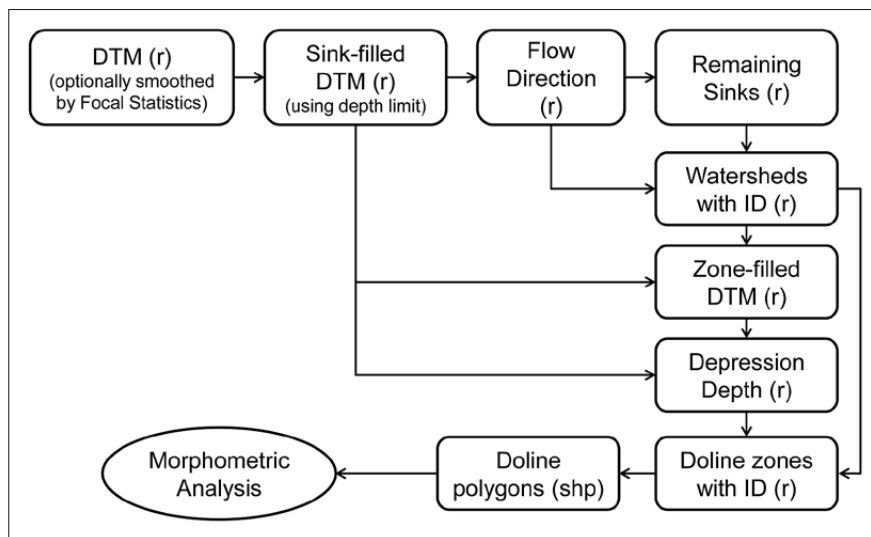
Fig. 2: Flow chart of doline delineation algorithm. r: raster; shp: shape format.

TOPOGRAPHIC MAP BASED DOLINE DELINEATION

In Hungary, there are good quality 1:10,000 scale topographic maps (FÖMI 2003). Our field experiences confirmed that dolines of Aggtelek Karst are well represented on these maps because doline sizes are typically on the 1000 m² scale (95 % of dolines are larger than 433 m²), and we found that almost all dolines are marked in the maps. Here we note, that in case of other karst terrains, where dolines are smaller, even the 1:10,000 scale maps may lack a significant proportion of dolines.

We digitized dolines from these topographic maps using the classical outermost closed contour line method (like in Bauer 2015). In the comparison, these data were considered as a reference. We also digitized doline centres, and depth values were calculated as the difference between the elevation of the outermost contour and the elevation of the centre point. Later on in this paper, data derived manually from the topographic maps are referred to as "TOPO".

DTM-BASED DOLINE DELINEATION

Closed depressions frequently occur in DTMs usually called as sinks, or pits. In case of non-karst terrains, these are mostly errors due to interpolation or low resolution. Thus, when DTMs were first utilized to create hydrographic networks, algorithms were elaborated to remove these pits by filling the closed depressions up to the level of the lowermost point of their rim (Jenson & Domingue 1988; Quinn *et al.* 1991). However, in case of karst, there is a large number of natural closed depressions. Thus, the above algorithms can be smartly used to identify sinks and fill only the DTM artefacts. It can be done by determining a depth limit and filling only the depressions, which are shallower than this limit. However, the choice of this limit is not unambiguous; we will discuss this question later. We carried out the analysis by ESRI ArcGIS 10.1 software, and our method is similar to the methodology used by the authors mentioned in the Introduction. Here we present the steps of the doline delineation algorithm using ESRI terminology (Fig. 2).

1. Smoothing of small errors by the application of a mean filter ("focal statistics"; applied only for the LiDAR DTM, using a 5-cell radius circular filter).
2. Filling of sinks (using different depth limits), the result is the "sink-filled DTM".
3. Determination of flow directions based on the sink-filled DTM.
4. Identification of the remaining sinks (deeper than the depth limit). A somewhat surprising result of this algorithm that sink points are usually found in pairs, but it does not cause a problem, because paired sink points have the same ID.
5. Delineation of watersheds using the remaining sink points.
6. Filling of the depressions up to the level of the lowermost point of their rim ("zonal fill")
7. Calculation of the difference between the zonal-filled DTM and the sink-filled DTM ("depression depth").
8, Areas with larger than zero difference are defined as dolines.
9. Dolines are converted to polygons for further analysis.
10. Doline geometrical properties (area, perimeter) are determined by standard methods ("calculate geometry"), other properties (length, width, axis orientation) by "zonal geometry", which uses a fitting ellipse method. The 10th step is equally applied to the TOPO dataset.

DTM DATA SOURCES

First, we used all digitized contour lines from the 1:10,000 scale topographic maps and interpolated a 10 m cell size DTM using kriging algorithm (with a simple linear variogram model). Kriging is able to calculate elevation values out of the data elevation range, which is very reasonable at convex summits and ridges and also in valley bottoms. However, depending on the compound geometry of contour lines, the interpolation process may result artefacts, namely holes at the valley bottoms. It must be taken into consideration when dolines are delineated. Hydrologic enforcing interpolation algorithms cannot be used in our case because they would fill natural sinks (dolines) as well. The above presented doline recognition algorithm was applied for the DTM created by kriging; data derived from this DTM are hereafter referred to as "KRIG".

Second, a LiDAR DTM was created of LiDAR data. The data acquisition was carried out in August 2013 by Envirosense Hungary Ltd ordered by Aggtelek National Park, using Leica ALS-70 HP (LiDAR) and Leica RCD 30 RGBN (supporting camera). For preprocessing, classification and interpolation of the leaf-on raw data OPALS software (Mandlburger *et al.* 2009; Otepka *et al.* 2012; Pfeifer *et al.* 2014) was used. Ground points were selected by robust filtering (with resulting point density 2 points/m^2) and interpolated to create a 2.5 m/px resolution DTM to cope with the lower density of ground points due to the leaf-on data. As for the interpolation, we used the moving plane algorithm of OPALS, that is a quick gridding method applicable for handling large amount of LiDAR data points. The interpolation resulted in some missing data patches, but mainly on steeper slopes and valley sides, therefore doline calculation is not considerably affected by this error. In order to correct small errors and to fill pixel-size gaps, a 5-pixel median filter was applied at first pass, and a 15-pixel median filter at second pass. The doline recognition algorithm was applied to the LiDAR-derived DTM; these dolines are hereafter referred to as "LiDAR" dataset.

RESULTS AND DISCUSSION

SENSITIVITY OF THE DOLINE RECOGNITION METHOD TO THE DEPTH LIMIT

Running the algorithm on the raw DTMs, we got 29,297 sinks for LiDAR and 1756 sinks for KRIG. It is why we applied first a smoothing filter for the LiDAR DTM. Thereafter, we changed the depth limit from 0.25 m to 1.5 m at 0.25 m increments. Our results (Tab. 1, Fig. 3) show that the number of depressions (hence the calculated doline densities) decreases as the depth limit increases, but this decrease is steeper in case of KRIG DTMs. The number

Tab. 1: Statistics of depression numbers with changing depth limit (gray marks the depth limit accepted as optimal). It is noted that when two small DTM-derived dolines are found in one TOPO doline (see Fig. 3c), then both DTM-derived dolines are accepted as TPs. Due to similar configurations, the sum of TP and FN is not exactly the same for all rows.

| DTM	Depth limit (m)	Number of depressions	Resulted doline density (km^{-2})	in TOPO & in DTM (TP)	in DTM, not in TOPO (FP)	in TOPO, not in DTM (FN)
KRIG	0.25	1391	15.2	1056	335	63
	0.50	1258	14.5	1025	233	76
	0.75	1176	14.0	998	178	93
	1.00	1115	13.6	981	134	103
	1.25	1043	13.1	948	95	126
	1.50	996	12.6	920	76	146
LiDAR	0.25	1235	16.1	1088	147	65
	0.50	1167	15.5	1070	97	70
	0.75	1111	14.9	1044	67	82
	1.00	1040	14.0	996	44	107
	1.25	1037	14.0	996	41	110
	1.50	1005	13.6	972	33	124
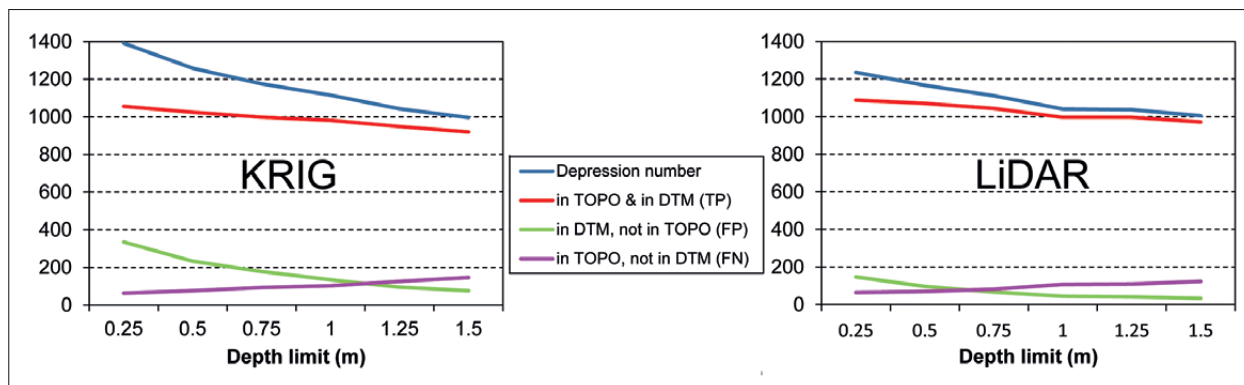
Fig. 3: Number of true and false dolines as a function of depth limit (TP: true positive; FP: false positive; FN: false negative).

of depressions existing in the DTM but not found in the TOPO reference data (Type I error, false positives, FP) also decreases with growing depth limit, and this gap between the DTM-derived and the reference TOPO data is circa 2.5 times higher in case of KRIG. On the other hand, the number of properly recognised dolines (true positives, TP) also decreases with increasing depth limit. Unfortunately, the Type II error, the number of TOPO dolines unidentified by the DTM-based method (false negatives, FN) increases with growing depth limit. Therefore, there is not an absolutely optimal solution in choosing the depth limit.

We think that the high number of false negatives is less favourable, because this way we lose a certain number of dolines from the morphometrical analysis. Furthermore, the false positives can be filtered out using other methods in a later step. This exclusion can be done based on morphometrical properties of FPs (Carvalho *et al.* 2013; Zhu *et al.* 2014) or by delineating terrains

where karst dolines may occur (area of interest), excluding FP depressions where dolines do not exist (Carvalho *et al.* 2013).

Taking into consideration these facts and options, we selected 1 m as the best depth limit for KRIG DTM, and 0.5 m as the best depth limit for LiDAR DTM. Further on, we applied the second option, that is, we delineated the doline-dotted areas of Aggtelek Karst, and in the further analysis we used only dolines found in these areas. In fact, some dolines do exist out of these areas, but in a very limited number. On the contrary, a large number of false dolines are found out of these areas, especially at valley bottoms (Fig. 4), due to interpolation errors, but also there are some true depressions which are of non-karstic origin. The doline densities of the final selection are slightly higher for the LiDAR dataset (15.5 km^{-2}) and slightly lower for the KRIG dataset (13.6 km^{-2}) with respect to the TOPO dolines (14.7 km^{-2}).
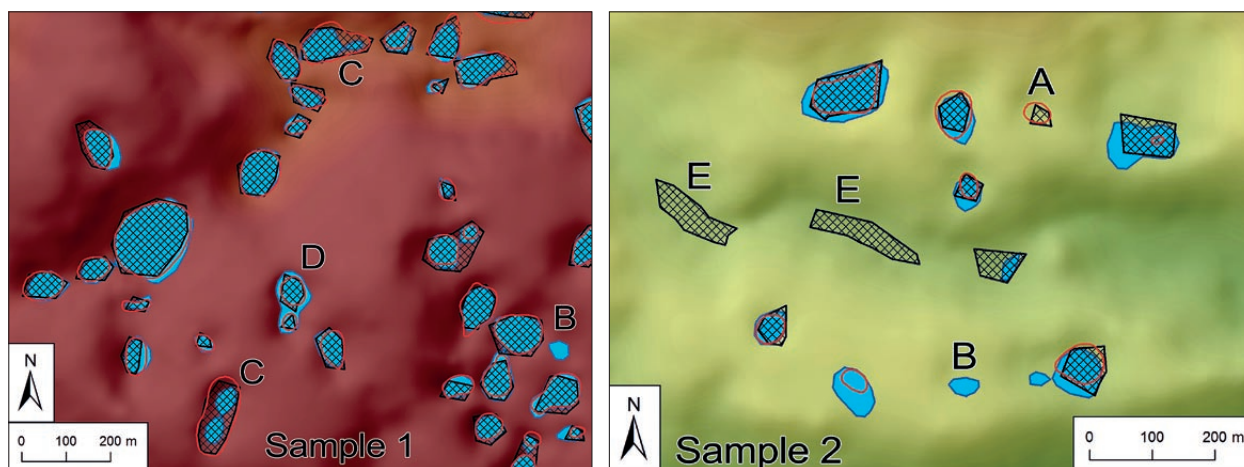

Fig. 4: Comparison of doline delineations on two map excerpts (S1 and S2 in Fig. 1). blue: LiDAR; crosshatched: KRIG; red outline: TOPO. A: doline not recognised by LiDAR; B: doline not recognised by TOPO; C: doline divided into two by LiDAR. D: two dolines merged by LiDAR; E: false doline at valley bottom.

Tab. 2: Most important statistics of doline features. The number of included dolines are: 1074 for TOPO, 995 for KRIG and 1136 for LiDAR.

	TOPO	LiDAR	KRIG	TOPO	LiDAR	KRIG
	AREA (m²)			**LENGTH (m)**		
Average	5962	6415	7295	91	95	104
Median	3304	3760	4236	76	81	87
Standard deviation	10089	10136	12472	62	60	66
Minimum	100	167	68	13	18	9
Maximum	200243	196509	250219	811	819	887
Skewness	126	124	133	42	46	44
	DEPTH (m)			**DEPTH/DIAMETER**		
Average	7.1	7.8	8.7	0.09	0.10	0.10
Median	6.5	6.7	7.5	0.09	0.10	0.10
Standard deviation	5.4	5.3	5.9	0.05	0.04	0.05
Minimum	1.0	0.6	0.2	0.01	0.01	0.01
Maximum	35.0	30.3	32.9	0.41	0.27	0.61
Skewness	17.1	15.4	12.7	14.06	3.99	17.17
	ELONGATION			**CIRCULARITY**		
Average	1.50	1.46	1.53	0.90	0.87	0.77
Median	1.39	1.37	1.41	0.93	0.89	0.78
Standard deviation	0.44	0.36	0.45	0.10	0.09	0.09
Minimum	1.01	1.01	1.00	0.29	0.31	0.37
Maximum	6.22	4.01	5.14	0.99	0.98	0.94
Skewness	41.33	27.68	33.11	-29.28	-26.90	−14.39

Two sample maps are presented to compare how the different methods delineate dolines (Fig. 4). It is obvious that LiDAR and TOPO shapes are finer than KRIG dolines, but in general, doline locations and forms are quite similar to each other. At some places, it occurs that a single TOPO doline is divided into two dolines in the DTM-derived datasets, and one can find examples for the opposite, too. Some small size dolines are missing from either the TOPO, or the KRIG or the LiDAR dataset. Nevertheless, these configurations are infrequent.

STATISTICAL COMPARISON OF DOLINE POPULATIONS

Standard statistics of doline morphometric properties can be seen in Tab. 2. These values were calculated taking into consideration all dolines found on the doline-dotted areas. In addition, we spatially joined dolines of the different databases and calculated linear correlations between the joined doline datasets. These correlations are presented for all pairs (TOPO–KRIG, TOPO–LiDAR, KRIG–LiDAR) in Tab. 3. Finally, the orientation of doline axes were calculated and presented in rose diagrams.

The planimetric area (simply "area" in the followings) is one of the most important measures of dolines. The statistical distribution of area usually follows a lognormal distribution, i.e. the logarithm of area is normally distributed (Telbisz 2001; Gao *et al.* 2005; Plan & Decker 2006; Telbisz *et al.* 2011). The lognormal distribution is the typical outcome of processes in which relative growth rate is independent of size. In the present study also, we found that area distributions are lognormal for TOPO, KRIG and LiDAR data alike (Fig. 5). It is confirmed by the Kolmogorov–Smirnov test as well (DN_{TOPO}=0.0311, P_{TOPO}=0.2490; DN_{KRIG}=0.0169, P_{KRIG}=0.9393; DN_{LiDAR}=0.0169, P_{LiDAR}=0.9099, all *P*-values are greater than 0.05, which means that the distributions can be adequately modeled by a lognormal distribution). Although the distributions are similar, there are certain differences in the distribution parameters: the TOPO dolines are significantly smaller then DTM-based dolines. It is due to the fact that the outermost closed contours define a lower elevation than the lowermost point of the edge of the closed depression, therefore the outermost closed contours encompass a smaller area than

Tab. 3: Linear correlations between spatially joined doline datasets.

	Parameter	TOPO–KRIG	TOPO–LIDAR	KRIG–LIDAR
HORIZONTAL SIZE	Area	0.9250	0.9438	0.9369
	Length	0.8799	0.9143	0.8993
	Perimeter	0.8907	0.9189	0.9179
VERTICAL DIMENSION	Depth	0.8971	0.8652	0.8764
	Depth/diameter	0.8392	0.7428	0.7700
SHAPE	Circularity	0.4955	0.7457	0.5689
	Elongation	0.6470	0.7425	0.6927
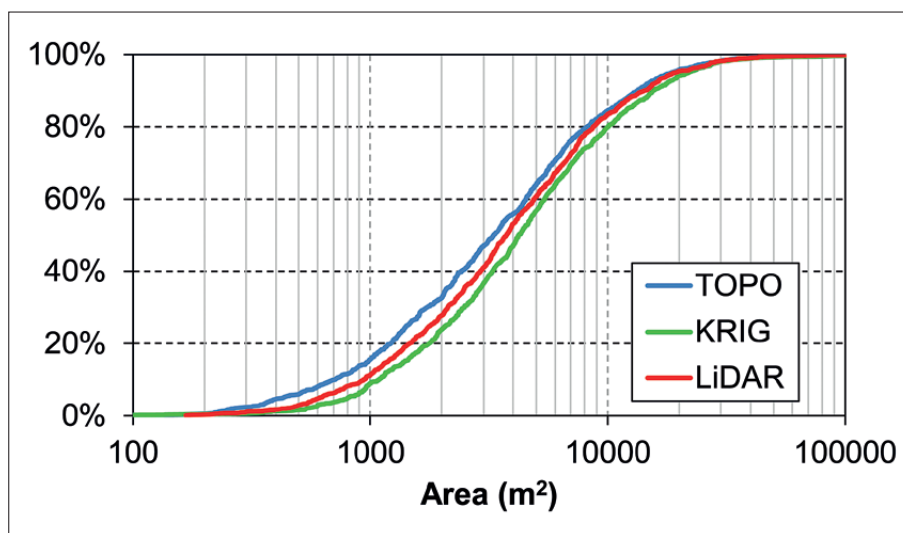
Fig. 5: Cumulative distributions of doline area.

the dolines delineated by using the fill method. Further on, KRIG dolines are even larger than LiDAR dolines. It is the result of grid resolution, because there are much tinier dolines in the LiDAR data, which reduces both the median and mean values. As for the spatially joined dolines, we found close linear correlations (r>0.925 for all pairs) between area values, which means that each method is almost equally appropriate for calculating planimetric area.

In each database, perimeter, length and width are in close multiplicative relationship with area (r>0.98). It is due to the fact that most dolines have a relatively simple elliptical or subcircular shape. Consequently, the above area statements (lognormal distribution, etc.) are more or less true for these parameters as well. Nevertheless, these characteristics (perimeter, length, width) are less robust; therefore the correlations between the joined doline datasets are slightly lower for these parameters (r≈0.9).

Depth is also a measure of doline size. At first, it looks natural that when conditions are similar, solution dolines may grow proportionally into horizontal and vertical dimensions. However, it is experienced, that cor-

relation between area and depth is usually smaller (in the present case, r=0.74 for LiDAR dolines). Moreover, the distribution of depth is not lognormal, but a gamma-type distribution (Fig. 6) confirmed by the Kolmogorov–Smirnov test (DN_{TOPO}=0.1541, P_{TOPO}=0.000; DN_{KRIG}=0.0414, P_{KRIG}=0.0667; DN_{LiDAR}=0.0231, P_{LiDAR}=0.5772, P-values for KRIG and LiDAR are greater than 0.05, which means that the distributions can be adequately modeled by a gamma distribution). Here again, DTM-derived dolines are deeper for the same reasons as their areas are larger. It is less obvious why KRIG dolines are significantly deeper than LiDAR dolines. The key is the kriging interpolation, which overdeepens the closed depressions resulting larger depth values. Another reason is that LiDAR data contain more small dolines. Evidently, we can accept the LiDAR depth as the best approximation of doline depth, because of measured point density and better grid resolution. Moreover, data reality is also reflected in the smoothest depth quantile curve of LiDAR. The staircase-like distribution of TOPO depth is due to the fact that doline depth read from topographic maps is quantized by the contour interval, it is why the K-S test rejects the gamma distribution for TOPO depth. As for
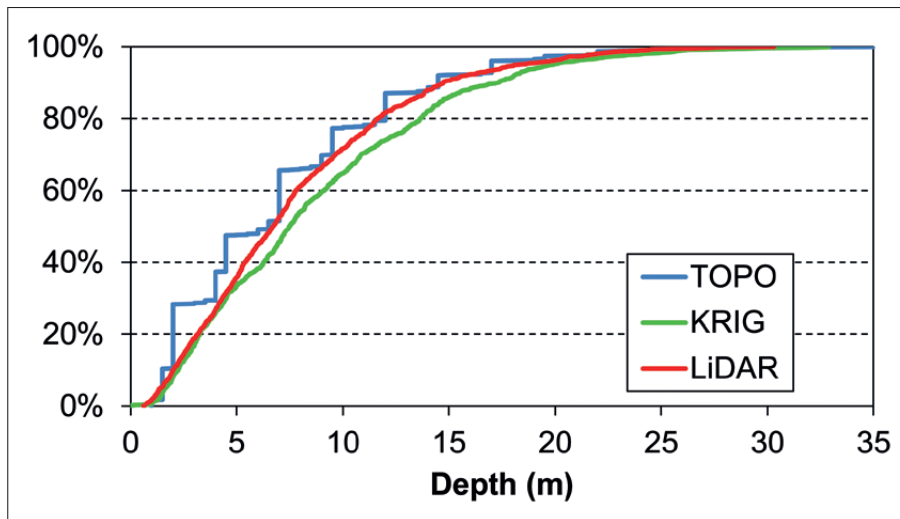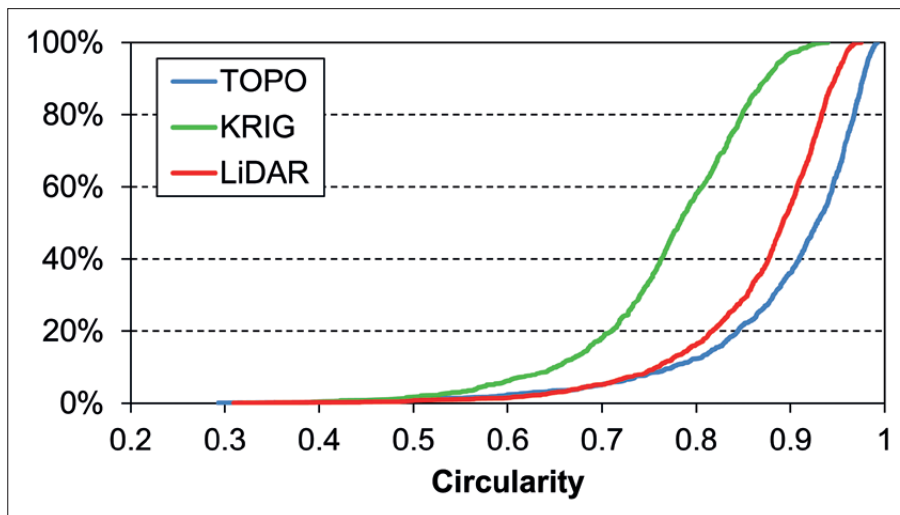
Fig. 6: *Cumulative distributions of doline depth.*

Fig. 7: *Cumulative distribution of doline circularity.*

the joined dolines relationship strengths, we get slightly lower correlations, than in the previous cases, but these values are still relatively high ($r \approx 0.87$), meaning that in spite of the above differences, depth can be satisfactorily determined by any of the methods if one takes into consideration the limitations of TOPO or KRIG datasets. On the other hand, depth-diameter ratios, which reflect the vertical proportions of dolines are less reliable in case of TOPO or KRIG, since correlations with LiDAR data are lower ($r \approx 0.75$). Here we note that depth-diameter ratios are important in discriminating dolines by their genesis (cf. Ford & Williams 1989).

Another group of morphometric parameters is in connection with the planimetric shape of dolines. Elongation, i.e. length-width ratio, simply expresses how elongated a doline is. It is very common that dolines are elongated along tectonic fractures, but in some cases doline elongation is determined by the antecedent valleys, which in turn can be constrained by the general-

ized aspect of the trend surface. As for elongation, the empirical distributions and the main statistics are quite similar using any of the methods. However, when joined dolines are considered, the correlations are only moderately strong (r between 0.64 and 0.74).

Circularity (C) relates the same area circle perimeter to the actual perimeter. It is calculated by the following formula: $C = 4 \cdot \pi \cdot Area / Perimeter^2$. Circularity is a more compound shape factor than elongation, because it is sensitive to both ellipticity and the tortuosity of the outline. Its value is 1 for a circle and smaller for elongated and indented shapes. This characteristic shows the largest differences (Fig. 7). Both distributions are quite different from each other, and the correlations between the joined datasets are the weakest (r between 0.5 and 0.75). TOPO dolines are the most circular that is obviously a matter of cartographic smoothing. On the other hand, KRIG dolines have a more angular shape due to the lower resolution of the KRIG DTM with respect to
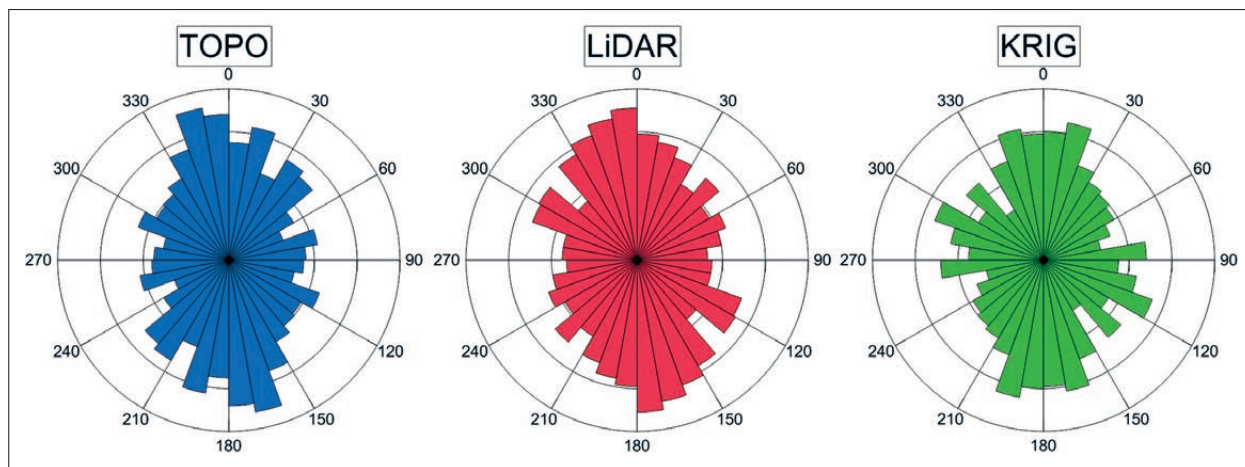
Fig. 8: Rose diagrams of doline long axes.

LiDAR DTM, which results that the circularity of KRIG dolines is unrealistically low. Thus, we argue that the LiDAR has a great advantage in the precise characterization of planimetric shape.

The orientations of doline long axes were compared by rose diagrams (Fig. 8). In this case, only dolines with elongation greater than 1.2 were taken into account. The rose diagrams demonstrate that the orientation of dolines are similar for all datasets with a peak at around 350°, and a secondary peak at around 300°, which conform in general to tectonic directions (Bárány-Kevei & Mezősi 1993) and to the general aspect of plateaus (Telbisz 2010). Minor differences are that the main peak is more to the north in KRIG, and the secondary peak is hardly visible in TOPO.

CLUSTERING OF DOLINES BY SLOPE CHARACTERISTICS

Slope histograms provide a characteristic fingerprint of landforms, and are suitable for landform classification, as

well as for object recognition (Favalli *et al.* 1999, Székely *et al.* 2002, Podobnikar & Székely 2015). DTM-derived slope values are dependent on grid resolution (Kienzle 2004), thus the high resolution LiDAR dataset is preferable in slope histogram calculation. In the followings, we represent how the LiDAR dataset can be used for a slope analysis of doline morphometry. However, this analysis is shown very briefly due to the limitations of paper length.

First, we determined slope histograms for all dolines using 1° class intervals. Second, we ran a hierarchical cluster analysis for doline slope histograms. Based on the dendrogram, we determined 9 classes. The main parameters and the mean slope histograms of the resulted clusters are presented in Tab. 4 and Fig. 9.

Before examining the clusters, we note that most dolines of Aggtelek Karst are of solution origin. However, there are several factors, which cause differences in doline forms, namely, whether the doline is found on a plateau or in a valley (Bárány-Kevei & Mezősi 1993),

Tab. 4: Main parameters of doline clusters based on slope distributions.

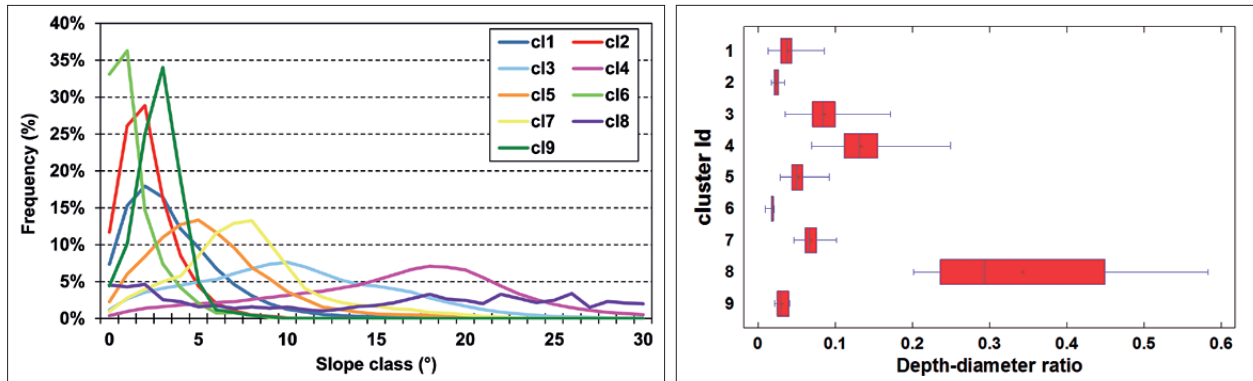| Cluster Id	Number of dolines	Area Median (m²)	Slope histogram	
			Mode	Kurtosis
cl1	64	2046	2°	mesokurtic
cl2	27	1371	2°	leptokurtic
cl3	342	3753	10°	platykurtic
cl4	525	4353	18°	platykurtic
cl5	137	1933	5°	mesokurtic
cl6	5	6436	1°	leptokurtic
cl7	56	2138	8°	mesokurtic
cl8	4	2161	2°	platykurtic
cl9	6	1562	3°	leptokurtic

Fig. 9: Slope histograms (left panel) and box-whisker plots of depth-diameter ratios (right panel) of doline clusters (cf. Table 4).

the relative elevation with respect to the karst water table, the clayey fill within the dolines (Zámbó 1998), the nonkarstic neighbourhood with allogenic water recharge (Jakucs 1956), the dip of limestone strata, etc. The spatial pattern of clusters is in connection with these factors.

The three most populated clusters are 3, 4 and 5. Cluster 4 contains dolines with the steepest slopes. Based on the histograms (Fig. 9), we can state that the typical hillslopes of these vertically well-developed dolines are 18°. The other more populated clusters include dolines with gentler typical hillslopes: 10° for cluster 3, and 5° for cluster 5. Considering the spatial distribution of clusters, one can observe that the most homogeneous part is Unit 6 (the eastern part of Alsó-hegy), where the steep-sided cluster 4 dolines are the most widespread. It is due to the fact, that this plateau is the most elevated (in the local context), with clear tectonic boundaries, with high dip angle strata, and the karst water table is relatively deep with respect to the surface. The effect of the former valley network on doline evolution is less significant here. Consequently, the deepening of dolines was relatively

intense in this area. The same is true for the southern part of Unit 2 (Nagyoldal). On the contrary, the most heterogeneous part is Unit 8 (Jósvafő plateau), a partly closed basin (supposed to be a polje in an earlier geologic period), which has a hydrographic exit today. It is at low elevation, close to the karst water table, segmented by several dry valleys. These factors led to the formation of variegated morphometric doline types. A large number of relatively low slope dolines (of clusters 1, 2 and 5) are found in Units 3 and 4, where dolomitic formations are present, and at the margins of the karst, where the allogenic discharge was more important during recent landform evolution.

It is remarkable that this clustering well differentiates dolines by their depth-diameter ratios as testified by Fig. 9, which shows the strength of this classical doline morphometrical parameter. However, as it was demonstrated in the previous subchapter, the LiDAR has its advantages in the calculation of depth-diameter ratios, too.

CONCLUSIONS

The automated doline delineation method performed well in this study area for both the KRIG and the LiDAR-derived DTMs. However, the depth limit influences the number of closed depressions, and the optimal threshold depends on the actual terrain characteristics. Here, in this study, 0.5 m for the LiDAR and 1 m for the KRIG dataset proved to be the optimal threshold when we compared our data to the reference TOPO dataset.

In general, the morphometrical distributions were similar for all datasets, but the DTM-based methodology resulted larger dolines with respect to the classical outermost closed contourline method. The area-dependent

characteristics (length, width, perimeter) resulted very high correlations between the joined datasets. However, depth parameters were less correlated and the worse correlations (being still moderately strong) were observed between circularity values of the different datasets.

Slope histograms calculated from the LiDAR data resulted a meaningful clustering of dolines and these clusters were in close relationship with the distribution of the classical depth-diameter ratio.

Summing up, it is concluded that the present study area (and other karst terrains with similar sized dolines and good quality, 1:10,000 scale maps) can be

morphometrically well characterized even by the classical topographic methods, though finer results can be achieved for the depth and shape related parameters by using LiDAR data. On the other hand, for terrains, where doline sizes are typically smaller (e.g. high mountains, juvenile doline terrains, etc.), and/or where good maps are missing (on hardly accessible karsts, see Kobal *et al.* 2015), LiDAR data can be extremely useful in morphometric characterization of closed depressions. This also applies to terrains, where the formation of dolines is an active and fast process, like in Florida (Zhu *et al.* 2014).

ACKNOWLEDGEMENTS

REFERENCES

Angel, J.C., Nelson, D.O. & S.V. Panno, 2004: Comparison of a new GIS-based technique and a manual method for determining sinkhole density: An example from Illinois' sinkhole plain.- Journal of Cave and Karst Studies, 66, 1, 9−17.

Bárány Kevei, I. & G. Mezősi, 1993: New morphometrical parameters for explanation of karst development.- Acta Geogr. Szegediensis, 31, 27−33.

Bauer, C., 2015: Analysis of dolines using multiple methods applied to airborne laser scanning data.- Geomorphology, 250, 78−88. http://dx.doi.org/10.1016/j.geomorph.2015.08.015

Brinkmann, R., Parise, M. & D. Dye, 2008: Sinkhole distribution in a rapidly developing urban environment: Hillsborough County, Tampa Bay area, Florida.- Engineering Geology, 99, 169−184. http://dx.doi.org/10.1016/j.enggeo.2007.11.020

Čar, J., 2001: Structural Bases for Shaping of Dolines.- Acta Carsologica, 30, 2, 239−256.

Carvalho, O.A., Guimarães, R.F., Montgomery, D.R., Gillespie, A.R., Trancoso Gomes, R.A., de Souza Martins, É. & N.C. Silva, 2013: Karst depression detection using ASTER, ALOS/PRISM and SRTM-derived digital elevation models in the Bambuí Group, Brazil.- Remote Sensing, 6, 1, 330−351. http://dx.doi.org/10.3390/rs6010330

Cvijić, J., 1893: Das Karstphänomen. Versuch einer morphologischen Monographie.- Geographischen Abhandlung, Wien 3, 218−329.

Day, M.J., 1983: Doline morphology and development in Barbados.- Annales of the Association of American Geographers, 73/2, 206−219. http://dx.doi.org/10.1111/j.1467-8306.1983.tb01408.x

Denizman, C., 2003: Morphometric and spatial distribution parameters of karstic depressions, Lower Suwannee River Basin, Florida.- Journal of Cave and Karst Studies, 65, 1, 29−35.

Faivre, S. & P. Reiffsteck, 2002: From doline distribution to tectonics movements example of the Velebit mountain range, Croatia.− Acta Carsologica, 31, 1, 139−154.

Favalli, M., Innocenti, F., Pareschi, M.T., Pasquarè, G., Mazzarini, F., Branca, S., Cavarra, L. & A. Tibaldi, 1999: The DEM of Mt. Etna: geomorphological and structural implications.- Geodin. Acta (Paris), 12, 5, 279−290. http://dx.doi.org/10.1080/09853111.1999.11105350

Florea, L., 2005: Using state-wide GIS data to identify coincidence between sinkholes and geologic structure.- Journal of Cave and Karst Studies, 67, 2, 120−124.

Ford, D.C. & P.W. Williams, 1989: *Karst Geomorphology and Hidrology*.- London, Unwin Hyman, pp. 560.

Gaál, L. & P. Bella, 2005: Vplyv tektonických pohybov na geomorfologický vývoj západnej časti Slovenského Krasu (The influence of tectonic movements to the geomorphological development of the western part of Slovak Karst).- Slovenský Kras (Acta Carsologica Slovaca), 43, 17−36. (in Slovakian)

Gallay, M., Kaňuk, J., Petrvalská A. & Z. Hochmuth, 2013: Využitie údajov leteckého laserového skenovania vo výskume krasovej krajiny na Slovensku – na príklade východnej časti Slovenského krasu. (Using the airborne laser scanning data in studying the karst landscape of Slovakia – case study of the eastern part of the Slovak Karst).- Slovenský kras, 51, 1, 99–108. (in Slovakian)

Gams, I., 2000: Doline morphogenetic processes from global and local viewpoints – Acta Carsologica 29, 2, 123–138.

Gao, Y., Alexander, E.C. & R.J. Barnes, 2005: Karst database implementation in Minnesota: analysis of sinkhole distribution.- Environmental Geology, 47, 1083–1098. http://dx.doi.org/10.1007/s00254-005-1241-2

Gostinčar, P., 2013: The application of GIS methods in morphometrical analysis of dolines on limestone and dolomite bedrock.- 16th International Congress of Speleology Proceedings, Brno, 84–88.

Hevesi, A., 1991: Magyarország karsztvidékeinek kialakulása és formakincse I-II. (Evolution and landforms of karst terrains in Hungary).- Földrajzi Közlemények, 115, 1–2, 25–35 and 115, 3–4, 99–120. (in Hungarian)

FÖMI (Institute of Geodesy, Cartography and Remote Sensing in Hungary), 2003: *Hungarian topographic maps at scale 1:10.000 (EOTR).*- Budapest.

Jakucs, L., 1956: Adatok az Aggteleki hegység és barlangjainak morfogenetikájához. (Data for the morphogenesis of Aggtelek Karst and its caves).- Földrajzi Közlemények, 4, 1, 25–35. (in Hungarian)

Jenson, S.K. & J.O. Domingue, 1988: Extracting topographic structure from digital elevation data for geographic information system analysis.- Photogramm. Eng. Remote Sens., 54, 11, 1593–1600.

Kemmerly, P.R., 1982: Spatial analysis of a karst depression population: clues to genesis.- Geol. Soc. of America Bulletin, 93, 1078–1086. http://dx.doi.org/10.1130/0016-7606(1982)93%3C1078:saoakd%3E2.0.co;2

Kemmerly, P.R., 1986: Exploring a contagion model for karst-terrain evolution.- Geol. Soc. of America Bulletin, 97, 5, 619–625. http://dx.doi.org/10.1130/0016-7606(1986)97%3C619:eacmfk%3E2.0.co;2

Kienzle, S., 2004: The Effect of DEM Raster Resolution on First Order, Second Order and Compound Terrain Derivatives.- Transactions in GIS 8, 1, 83–111. http://dx.doi.org/10.1111/j.1467-9671.2004.00169.x

Kobal, M., Bertoncelj, I., Pirotti, F., Dakskobler, I. & L., Kutnar, 2015: Using Lidar Data to Analyse Sinkhole Characteristics Relevant for Understory Vegetation under Forest Cover – Case Study of a High Karst Area in the Dinaric Mountains.- PLoS ONE 10, 3, e0122070, doi:10.1371/journal.pone.0122070.

Less, Gy., 1998: Földtani felépítés. (Geology of Aggtelek National Park).- In: Baross, G. (ed.): *Az Aggteleki Nemzeti Park.* Mezőgazda Kiadó, pp. 26–66. (Budapest in Hungarian).

Mandlburger, G., Otepka J., Karel W., Wagner W. & N. Pfeifer, 2009: Orientation And Processing Of Airborne Laser Scanning Data (OPALS) – Concept and First Results of a Comprehensive ALS Software.- The International Archives of the Photogrammetry, Remote Sensing and Spatial Information Sciences, 38, Part 3/W8, 55–60.

Mezősi, G., 1984: A Sajó-Bódva köze felszínfejlődése (Landform evolution of the Sajó-Bódva interfluve).- Földrajzi Értesítő (Hungarian Geographical Bulletin), 33, 3, 181–205. (in Hungarian)

Mills, H.H. & D.D. Starnes, 1983: Sinkhole morphometry in a fluviokarst region: eastern Highland Rim, Tennessee, US.- Z. Geomorph, 27, 1, 39–54.

Móga, J., 1999: Reconstruction of the development history of karstic water networks on the Southern part of the Gömör-Torna Karst on the bases of ruined caves and landforms.- Acta Carsologica, 28, 2, 159–174.

Obu, J. & T. Podobnikar, 2013: Algoritem za prepoznavanje kraških kotanj na podlagi digitalnega modela reliefa (Algorithm for Karst Depression Recognition Using Digital Terrain Model).- Geodetski vestnik, 57, 2, 260–270. (in Slovenian) http://dx.doi.org/10.15292/geodetski-vestnik.2013.02.260–270

Orndorff, R.C., Weary, D.J. & K.M. Lagueux, 2000: Geographic Information Systems Analysis of Geologic Controls on the Distribution of Dolines in the Ozarks of South-Central Missouri, USA.- Acta Carsologica, 29, 2, 161–175.

Otepka, J., Mandlburger G. & W. Karel, 2012: The OPALS Data Manager – Efficient Data Management for Processing Large Airborne Laser Scanning Projects.- ISPRS Annals, Comm. III, 1–3, 153–159. http://dx.doi.org/10.5194/isprsannals-i-3-153-2012

Pahernik, M., 2012: Prostorna gustoća ponikava na području Republike Hrvatske (Spatial Density of Dolines in the Croatian Territory).- Hrvatski Geografski Glasnik, 74, 2, 5–26. (in Croatian)

Pardo-Igúzquiza, E., Durán J.J. & P.A. Dowd, 2013: Automatic detection and delineation of karst terrain depressions and its application in geomorphological mapping and morphometric analysis.- Acta Carsologica, 42, 1, 17–24. http://dx.doi.org/10.3986/ac.v42i1.637

Petrvalská, A., 2010a: Vývoj názorov na vznik a genézu zarovnaných povrchov Slovenskeho Krasu (Development of conceptions concerning origins and genesis of planation surface of Slovak karst).- Acta Geographica Universitatis Comenianae, 54, 1, 81–99. (in Slovakian)

Petrvalská, A., 2010b: Morfometrická analýza závrtov na príklade Jasovskej planiny, Slovenský kras. (Morphometric analysis of dolines on Jasovská plateau, Slovak Karst).- Geomorphologica Slovaca et Bohemica, 10, 1, 33–44. (in Slovakian)

Petrvalská, A., 2012: Výsledky morfologického mapovania závrtov na Jasovskej planine v Slovenskom krase. (Morphometric mapping results about the Jasovská plateau, Slovak Karst).- Slovenský kras, 50, 2, 63–71. (in Slovakian)

Pfeifer, N., Mandlburger, G., Otepka, J. & W. Karel, 2014: OPALS – A framework for Airborne Laser Scanning data analysis.- Computers, Environment and Urban Systems, 45, 125–136. http://dx.doi.org/10.1016/j.compenvurbsys.2013.11.002

Plan, L. & K. Decker, 2006: Quantitative karst morphology of the Hochschwab plateau, Eastern Alps, Austria.- Z. Geomorph. N.F., Suppl.-Vol. 147, 29–54.

Podobnikar, T. & B. Székely, 2015: Towards the automated geomorphometric extraction of talus slopes in Martian landscapes.- Planetary and Space Science, 105, 148–158. http://dx.doi.org/10.1016/j.pss.2014.11.019

Quinn, P., Beven, K., Chevallier, P. & O. Planchon, 1991: The prediction of hillslope flow paths for distributed hydrological modelling using digital terrain models.- Hydrol. Proc., 5, 59–79. http://dx.doi.org/10.1002/hyp.3360050106

Rahimi, M., & E.C. Alexander, 2013: Locating sinkholes in LiDAR coverage of a glacio-fluvial karst, Winona County, MN.- Thirteenth Multidisciplinary Conference on Sinkholes and the Engineering and Environmental Impacts of Karst: Carlsbad, National Cave and Karst Research Institute, Symposium 2, 469–480.

Sauro, U., 2003: Dolines and sinkholes: aspects of evolution and problems of classification.- Acta Carsologica, 32, 2, 41–52.

Šušteršič, F., 1994: Classic dolines of classical site.- Acta Carsologica, 23, 10, 123–154.

Székely, B., Reinecker, J., Dunkl, I., Frisch, W. & J. Kuhlemann, 2002: Neotectonic movements and their geomorphic response as reflected in surface parameters and stress patterns in the Eastern Alps.- in: Cloething Sierd A.P.L., Horváth, F., Lankreijer, A. & G. Bada (eds.): *Neotectonics and seismicity of the Pannonian basin and surrounding orogens.* EGU Stephan Mueller Special Publication Series, 3, 149–166. http://dx.doi.org/10.5194/smsps-3-149-2002

Telbisz, T., 2001: Új megközelítések a töbör-morfológiában az Aggteleki-karszt példáján (New perspectives in doline morphometry – Aggtelek Karst as an example).- Földrajzi Közlemények, 125 (49), 1–2, 95–108. (in Hungarian)

Telbisz, T., 2011: Large-scale relief of the Slovak Karst and Aggtelek Karst (Gömör-Torna/Gemer-Turňa Karst) – a DEM-based study.- Hungarian Geographical Bulletin, 60, 4, 379–396.

Telbisz, T., Dragušica, H. & B. Nagy, 2009: Doline Morphometric Analysis and Karst Morphology of Biokovo Mt (Croatia) based on Field Observations and Digital Terrain Analysis.- Croatian Geographical Bulletin, 71,2, 2–22.

Telbisz, T., Mari, L. & L. Szabó, 2011: Geomorphological characteristics of the Italian side of Canin Massif (Julian Alps) using digital terrain analysis and field observations.- Acta Carsologica, 40, 2, 255–266. http://dx.doi.org/10.3986/ac.v40i2.10

Veress, M., 2008: Adalékok az Aggteleki-fennsík völgyeinek fejlődéséhez (New data for the evolution of Aggtelek plateau valleys).- Karszt és Barlang, 2008, 1–2, 3–12. (in Hungarian)

Vincent, P.J., 1987: Spatial dispersion of polygonal karst sinks.- Z. Geomorph, 31, 1, 65–72.

Williams, P.W., 1971: Illustrating morphometric analysis of karst with examples from New Guinea.- Z. Geomorph, 15, 1, 40–61.

Zámbó, L., 1998: Felszínalaktani jellemzés. (Geomorphology of Aggtelek National Park).- in: Baross G. (ed.): *Az Aggteleki Nemzeti Park*. Mezőgazda Kiadó, pp. 70–96. (Budapest in Hungarian).

Zboray, Z. & I. Bárány Kevei, 2004: Domborzatértékelés a Bükk-fennsíkon légifelvételek felhasználásával. (Relief evaluation of Bükk plateau using aerial photographs).- Karsztfejlődés 9, 207–213. (in Hungarian)

Zhu, J., Taylor, T.P., Currens, J.C. & M.M. Crawford, 2014: Improved karst sinkhole mapping in Kentucky using LiDAR techniques: a pilot study in Floyds Fork Watershed.- Journal of Cave and Karst Studies, 76, 3, 207–216. http://dx.doi.org/10.4311/2013es0135